CHEMISTRY
A European Journal

A Journal of
ChemPubSoc Europe

Accepted Article

Title: Enhanced Peroxidase-like Properties of Graphene-hemin Composite Decorated Au Nanoflower and Application of Electrochemical Aptamer Biosensor for Detection of K562 Cells

Authors: Jing Liu, Meirong Cui, Li Niu, Hong Zhou, and Shusheng Zhang

To be cited as: *Chem. Eur. J.* 10.1002/chem.201604354

Link to VoR: http://dx.doi.org/10.1002/chem.201604354

Supported by
ACES

WILEY-VCH

10.1002/chem.201604354

WILEY-VCH

Enhanced Peroxidase-like Properties of Graphene-hemin Composite Decorated Au Nanoflower and Application of Electrochemical Aptamer Biosensor for Detection of K562 Cells

Jing Liu,[a] Meirong Cui, [a,b] Li Niu,[a] Hong Zhou,*[a] and Shusheng Zhang*[a]

Abstract: Graphene composite connected with hemin and gold nanoparticles showing better performance for hydrogen peroxide decomposition compared that of three components alone or duplex hybrid complex. Our previous studies showed that, the morphology of the Au nanoparticles may greatly influence the catalytic activity of graphene-family peroxidase mimetic. Recently, interestingly we found that Au nanoflower could in-situ grow and form on the surface of Hemin/RGO. And the prickly morphology of this Au nanoflower brought higher catalytic ability with enhanced kinetic parameter than traditional Au nanoparticles which showed smooth surface on the surface of graphene. Therefore based on this discovery, a smart electrochemical aptamer biosensor for K562 cells was further presented with good performance in selectivity and sensitivity attributed to the excellent mimetic peroxidase catalytic activity of this newly-synthesed Au nanoflower decorated graphene-hemin composites (H-RGO-Au NFs).

Introduction

Aptamer-based biosensor is a brilliant prospect for the detection of disease related protein, small molecules, and even cells due to its high bio-affinity, fine steric effect, and excellent selectivity. Aptamers are a kind of artificially selected nucleic acid sequences holding high specificity or affinity toward some small molecules, proteins, and cells.[1-4] Comparing with large antibodies, aptamers usually hold a small size, a tunable sequences which provides much convenience for clinical diagnostics. Recently, various aptamer based cyto-sensors have been reported for cancer research *via* chemiluminescence,[5,6] electrochemistry or electrochemiluminescence,[7-9] fluorescence,[10-12] and so on. These conventional methods are faced with problems which are mainly complicated and with dissatisfactory sensitivity.

Compared with natural enzymes, peroxidase mimetic, as a newly-developing material, has attracted wide interest due to its excellent properties, such as high stability, good flexibility for decoration and satisfactory catalytic efficiency. Moreover, it showed low costs of preparation, purification and storage, which greatly enlarged the widespread applications in many fields.[13] Up to now, many nanomaterial-based peroxidase mimetics were reported, such as noble metal based nanoparticles,[14-16] Au clusters,[17] magnetic metal Fe_3O_4,[18-20] graphene oxide,[21] graphene quantum,[22] porphyrin-based composite,[23] etc.

Hybrid nanomaterials as a new generation of peroxidase mimetics are promising materials due to some particular properties during biosensing with high catalysis activity. Thereinto, hybrid peroxidase mimetics based on soluble graphene oxide (GO) have triggered much attention which have been extensively studied during heterogeneous catalytic processes with larger specific surface areas and higher adsorption capacity provided by GO. [24-26] And after Au NPs was reported to exhibit high intrinsic peroxidase-like activity by Li and co-workers,[27] many studies of nanomaterials-based graphene-family peroxidase mimetics appeared.[28,29] For example, Qu's group[24] developed a composite of GO and gold nanoclusters which showed a higher peroxidase-like activity due to synergistic catalyst and could be employed for cancer cell detection. Another example is Weng and co-workers[30] further presented a composite connecting graphene with hemin and gold nanoparticles which showed better performance for hydrogen peroxide decomposition compared that of three components alone or duplex hybrid complex. Furthermore, in consideration of the positively-charged gold nanorod, we have designed a new material based on hemin modified graphene (H-RGO) and gold nanorods with enhanced catalytic activity as peroxidase mimetics compared with traditional Au nanoparties[31,32]. This maybe because the abundantly attached gold nanorods which could greatly improve its catalytic abilities compared with other graphene-family peroxidase mimetics. Inspired by this, the morphology of the Au nanopartles is expected to greatly influence the peroxidase-like catalytic activity.

Recently, interestingly we found that traditional Au nanoparticles could in-situ grow on the surface of H-RGO and further form Au nanoflower. And the prickly morphology of Au nanoflower brought higher catalytic ability than traditional Au nanoparticles which showed smooth surface on the surface of GO. The catalytic activity of three GO-family materials including previously-reported H-RGO-Au nanoparticles (H-RGO-Au NPs), H-RGO-Au nanorods (H-RGO-Au NRs), and newly-presented H-RGO-Au nanoflowers (H-RGO-Au NFs) was studied through enzyme kinetics experiments with H_2O_2 and TMB as substrates. Then the important kinetic parameters such as Michaelis constant (K_m) and maximal reaction velocity (V_{max}) were derived and compared among above three composite and natural enzyme HRP. A low K_m suggests a strong enzyme affinity to the substrates and vice versa[33,34]. By comparing above kinetic parameters, the newly-designed nanoflowers (H-RGO-Au NFs) showed most excellent properties as an artificial enzyme. Therefore, based on this novel material and aptamer technology, a smart electrochemical aptamer biosensor for K562 cells was

[a] Dr. J.Liu, M. R. Cui, Dr.L.Niu, Dr. H.Zhou,Prof. Dr. S. Zhang
Shandong Provincial Key Laboratory of Detection Technology for Tumor Markers, College of Chemistry and Chemical Engineering, Linyi University
Linyi 276005 (P. R. China)
E-mail:zhouhong830215@126.com
[b] M. R. Cui,
Collaborative innovation center of functionalized probes for chemical imaging in universities of Shandong, Shandong Normal University
Jinan 250014 (P. R. China)

Supporting information for this article is given via a link at the end of the document.

further presented with good performance in selectivity and sensitivity attributed to the excellent mimetic peroxidase catalytic activity of H-RGO-Au NFs (Scheme 1).

Employment of aptamer is a very simple method to specifically recognize particular kind cells (for example K562 cells as myelogenous leukemia line) via specific identification effect between the cells and the aptamer. Moreover, owing to the high electron transfer rate of graphene, the synergistic interaction from three components, and higher catalytic performance due to the prickly morphology of Au nanoflower, a low detection limit of 2 cells is achieved using this novel graphene-family hybrid gold nanoflowers-based peroxidase mimetics. The application of this kind of peroxidase mimetics is a promising approach for the construction of simple, biosensors for sensitive and selective detections of various analytes inside or outside of cells.

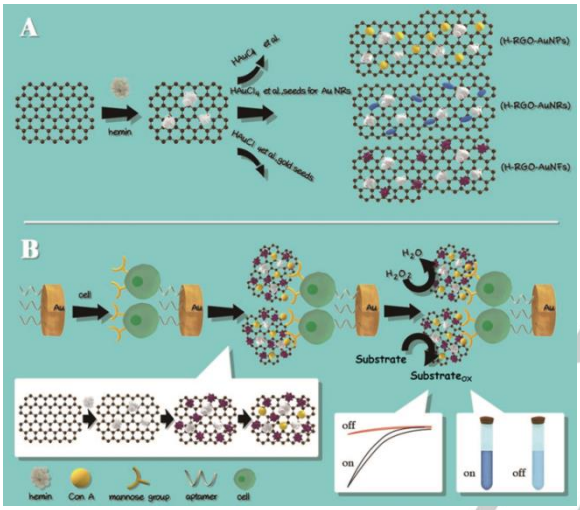

Scheme 1. Synthesis process of graphene-family ternary composites and aptamer biosensor for K562 cells.

Results and Discussion

Characterizations of newly-presented H-GO-Au NFs

Transmission electron microscopy (TEM) was first used to show the morphology of prepared composites. As showed in Figure 1A, a wrinkled and folded layer of GO changed as modified with hemin (A-1 and A-2), and after further modification with uniform 25 nm gold seeds (Figure.1A-3), an interesting nanofolwer morphology was found which were densely decorated on the surface of H-RGO (Figure. 1A-4). The diameter of this Au NFs is estimated to be around 75-100 nm and an obvious prickly morphology was presented from the formed Au nanoflower which was expected to improve its catalytic ability. Figure 1B was the comparison in UV-vis spectra before and after modification of gold nanofolwer on H-RGO. Also the UV-vis spectra of contrast group bare GO, hemin molecule were provided here. GO showed a peak at about 233 nm and a weak shoulder peak at 300 nm due to π-π * transitions of C=C band and n-π* transitions of C=O band, respectively. And due to Soret band and Q-bands of hemin, it presented a strong peak at 388 nm and a series of weak peaks from 500 to 700 nm. As to H-RGO, the maximum peak of the Soret band of hemin showed red-shifts from 388 to 413 nm, this maybe due to the adsorbed hemin molecule' π-π stacking interaction raised by porphyrin moiety and substrate graphene. And after formation of nanoflowers, a new absorption band is found at about 600 nm, which is identified as the plasmon band of Au nanoflower. This indicated the successful generation and attachment of Au nanoflower on the graphene-based substrate. Further Energy-dispersive analysis of X-rays (EDX) which could characterize the elemental composition of composite was also carried out presented in Figure. 1C). The result accords with that from TEM and UV measurements.

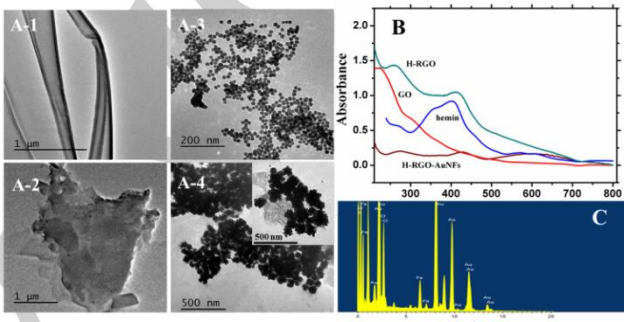

Figure 1. (A) TEM images of GO (A-1), H-RGO (A-2), gold seeds (A-3), and the as-synthesized ternary composite H-RGO-Au NFs (A-4); (B) UV/Vis absorption spectra of the GO, Hemin, H-GO, and H-RGO-Au NFs. insert of A-4 is the corresponding partly enlarged view of H-RGO-Au NFs; (C) EDX analysis of H-RGO-Au NFs.

Comparation in catalytic activity of H-RGO-Au NFs and other materials

Our previous study found that a new graphene-family material integrated by hemin and gold nanorods showing enhanced catalytic ability as peroxidase mimetics compared that of former duplex hybrid complex and even ternary graphene material (modified with hemin and gold nanoparticles) reported by Weng and co-workers. Then we deduced that the morphology of the Au nanopartles is expected to greatly influence the peroxidase-like catalytic activity. Therefore, three kinds of H-RGO-Au composites which hold different Au morphology (showed in Figure 2) were compared.

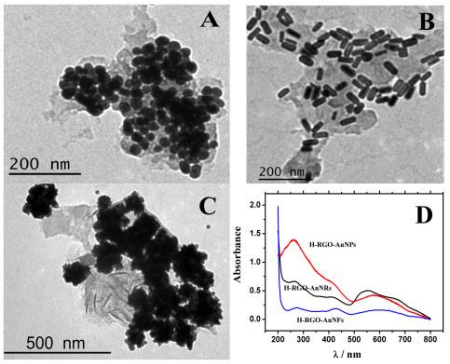

Figure 2. TEM images of as-synthesized H-RGO-Au NPs (A), H-RGO-Au NRs (B) and H-RGO-Au NFs (C), (D) is The comparison in UV−vis absorption spectra of these three materials.

To analyze the catalytic performance of these composites, kinetic parameters were obtained during enzyme kinetics experiments with TMB/H_2O_2 as substrates. Detailly, following experiments were conducted to find time-dependent absorbance changes at 652 nm by fixing the amount of one substrate and changing the other (Figure S1, Supplementary Information). To characterize the enzyme activity of newly-presented H-RGO-Au NFs as peroxidase mimics and former-reported H-RGO-Au NPs or H-RGO-Au NRs, the Michaelis-Menten curves were deduced as showed in Figure 3A, B. Then, according to the responsive oxidation rates changes with varying substrate concentrations, a Lineweaver-Burk plot could be obtained and showed in Figure 3 C, D with an excellent linear relationship. Based on this data, K_m and V_{max} as the most important kinetic parameters could be derived and presented in Table 1 from which the comparison of three kinds of H-RGO-Au ternary composite and frequently-used natural enzyme HRP was listed.

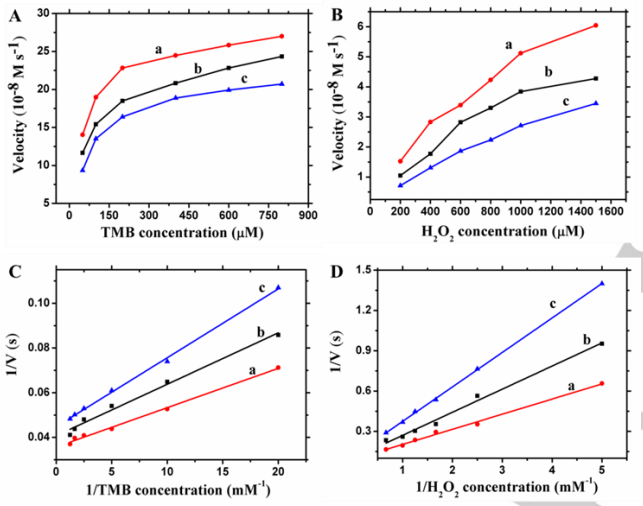

Figure 3. (A) The velocity (v) of the reaction changes in the presence of H-RGO-Au NFs (a), H-RGO-Au NRs (b), H-RGO-Au NPs (c) and different concentrations of TMB (H_2O_2 concentration was fixed at 10 mM); (B) The velocity (v) of the reaction changes in the presence of H-RGO-Au NFs (a), H-RGO-Au NRs (b), H-RGO-Au NPs (c) and different concentrations of H_2O_2 (TMB concentration was fixed at 600 mM); (C) Double reciprocal plots of activity of H-RGO-Au composites in the presence of different concentrations of TMB; (D) Double reciprocal plots of activity of H-RGO-Au in the presence of different concentrations of H_2O_2. Experiments were carried out in 0.02 M acetic acid-sodium acetate buffer (pH 4.0) using 0.7 μg mL^{-1} H-RGO-Au composite at 25℃.

K_m was the Michaelis-Menten constant which equaled to the substrate concentration when the reaction velocity reached half of V_{max}. And a low K_m was usually represented as a strong affinity of enzyme and vice versa.[33] While higher V_{max} obviously indicated higher catalytic velocity and enzyme activity. From Table 1, we could find that the apparent K_m value of three ternary composites with TMB or H_2O_2 as the substrate are significantly lower than that for HRP, suggesting that three kinds of H-RGO-Au composite all have a higher affinity for TMB or H_2O_2 than HRP.[37] Moreover, newly-designed H-RGO-Au NFs showed the lowest K_m value which is 1.4 times lower than that of H-RGO-Au NPs and 8.82 times lower than that of HRP with TMB as the substrate. And the performance of new H-RGO-Au NFs with H_2O_2 substrate is also impressive with lower K_m value compared with HRP or other H-RGO-Au composites.

Table 1. Comparison of the Kinetic Parameters of three kinds of H-RGO-Au composite and HRP[a].

Catalysts	Substrate	K_m (mM^{-1})	V_{max} (10^{-8} M s^{-1})
H-RGO-Au NPs	TMB	0.0687	22.31
H-RGO-Au NPs	H_2O_2	2.17	8.49
H-RGO-Au NRs	TMB	0.0564	24.52
H-RGO-Au NRs	H_2O_2	1.749	10
H-RGO-Au NFs	TMB	0.0492	28.49
H-RGO-Au NFs	H_2O_2	1.24	11.1
HRP[37]	TMB	0.434	10
HRP[37]	H_2O_2	3.7	8.71

[a] K_m is the Michaelis constant; V_{max} is the maximal reaction velocity.

This may be because of high surface-to-volume ratios of synthesed materials which could absorb reaction substrate efficiently.[38] Also, graphene could anchor hemin molecule and gold nanomaterial and concentrate the substrates in this region, and this may largely improve the catalytic ability of the composite.[39] Moreover among the synthesized three kinds graphene-Au family composite, H-RGO-Au NFs showed prickly morphology of Au nanoflower on the surface which is expected to further enlarge its surface-to-volume ratios and then improve the catalysis ability. As such, the V_{max} of graphene-Au family composite is also higher than that of other composite materials or natural enzyme HRP. Taken above together, attributing to the synergetic effect among substrate graphene, hemin and gold nanoparticles, as well as the particular morphology of gold nanoflower, the newly-presented ternary materials H-RGO-Au NFs showed a higher catalysis activity than that of previously reported catalysts. Besides this, the enlarged surface area of this RGO-family composite also provided promising applications for various biomolecules even cancer cells.

Preparation of aptamer bisensor using H-RGO-Au NFs

Two steps needed for the construction of aptamer bisensor were depicted in Scheme 1B. First, Con A/H-RGO-Au NFs was prepared at advance. Con A is a type of lectin, which could specifically recognize sugar epitopes and then showed the ability to specifically identify glycan on the surface of cells, especially tumor cells.[40-44] The cleaned gold electrode was modified with a layer of aptamer DNA molecules, then K562 cells could further modified on the electrode through discrimination reaction between aptamer DNA and K562 cells. After this, the previously prepared Con A/H-RGO-Au NFs complex could further specifically bind onto the surface of K562 cells. During this preparation of aptamer biosensor, the

introduced H-RGO-Au NFs composite not only hold enlarged surface area for sufficient Con A, but also showed high catalytic capability for H_2O_2 from which the concentration of K562 cells could be monitored. The prepared Con A linked H-RGO-Au NFs composite was characterized by UV spectrum. Data of UV spectrum of H-RGO-Au NFs composite with and without combination of Con A was showed in Figure S2 (Supplementary Information).

Some experimental conditions were further optimized to obtain the optimum performance of this biosensor. First the ratio of Con A/H-RGO-Au NFs was optimized during the step of preparation of Con A/ H-RGO-Au NFs complex. By changing the ratio of Con A /H-RGO-Au NFs from 1:2 to 2:1, the current response increased and decreased with a plateau at 1:1 (Figure 4A). Following this, incubation time as another important parameter for cells capture was investigated ranged from 20 min to 120 min. As showed in Figure 4B, the current was found to reach its maximum and became stable at 90 min. Therefore, 90 min and volume proportion at 1:1 of Con A/H-RGO-Au NFs were selected as optimal conditions for this sensing system.

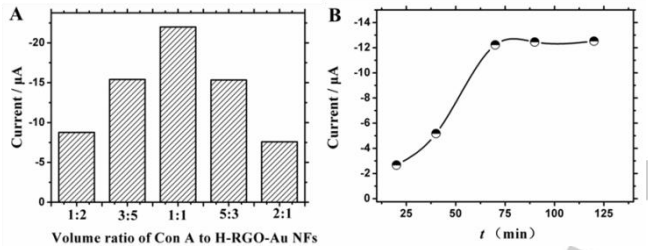

Figure 4. Current of cyclic voltammograms at -0.6V for analysis on (A) Volume ratio of Con A to H-RGO-Au NRs used for preparation of the biosensor; (B) different incubation time of Con A/ H-RGO-Au NFs and K562 cells.

Cytosensing for K562 cells

The performance of this biosensor for cell detection was evaluated under the treatment and without treatment of K562 cells. The aptamer DNA-modified gold electrode was treated with 1.0×10^4 cells mL^{-1} of target cells for 30 min. Then the electrode was rinsed and further immersed in Con A/ H-RGO-Au NFs complex for 90 min at 37℃. After this, current response of CVs between -0.6 V to 0 V at a scan rate of 10 mV s^{-1} was recorded, and the current value at -0.6 V was collected for analysis. The control experiment was conducted using the same steps just without the treatment of K562 cells. The results in Figure 5A showed that after the treatment of K562 cells, the response of the current at -0.6V was significantly enhanced compared with that of control group. Besides this electrochemical response, the colorimetric measurement was also employed. After immersing the electrode in 200 μL TMB/H_2O_2 substrate for 5 min, the solution color was observed and recorded by mobile phone (insert of Figure 5A). From this, an obvious color change could be found after the incubation of target cells which further confirmed that K562 cells could be detected using this designed biosensor.

Then, the quantitative range and sensitivity for K562 cells detection were tested under the optimal reaction conditions by changing K562 cell concentrations according to the protocol described in Scheme 1. K562 cell was known to express glycoprotein on its surface,[45] and then through the specific combination between Con A and the glycoprotein, Con A linked peroxidase mimetic H-RGO-Au NFs could bind onto the electrode surface. And this could result in an obvious catalytic current in H_2O_2 solution in the present of target cells. Moreover the current response was expected to change when using different K562 cells concentration due to different amount of glycan expressed.

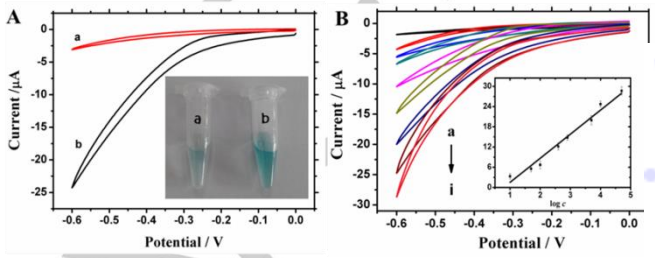

Figure 5. (A) Cyclic voltammograms of the prepared sensing electrode with (b and without (a) treatment of K562 cells in 2 mM H_2O_2. Insert is the representative photograph of above electrodes in TMB-H_2O_2 system. The photos were taken after 5 min reaction with peroxidase mimetic H-RGO-Au NFs modified electrodes with (b) and without (a) treatment of K562 cells; (B) (CV current at -0.6V versus different K562 cell concentrations (from a to i: 0, 10, 50, 100, 400, 800, 5.0×10^3, 1.0×10^4, 5.0×10^4 cells mL^{-1} respectively) in 2 mM H_2O_2. Potential: -0.6-0 V (*vs*. Ag/AgCl). Insert are plots of CV current at -0.6V *vs.* logarithm value of K562 cell concentration. The error bars were obtained from three parallel experiments.

From the data showed in Figure 5B, we could found that the current increased as K562 cells concentration increased from 0 to 5.0×10^4 cells mL^{-1}. Good linear relationships were demonstrated between catalysis current and logarithm of the concentration of K562 cells in above range (insert in Figure 5B). From this, a satisfactory detection limit of 10 cells mL^{-1} for K562 cells was achieved. Considering 200 μL test solution were used in the process of biosensing, extremely low detection limit of 2 K562 cells was realized and this may be attributed to the excellent catalytic performance and enlarged surface area of the prepared ternary composite. The linear regression equation was i (μA) = 7.23 log c-5.68 (R=0.98), where i is the current intensity obtained at -0.6 V and c is cell concentration (cells mL^{-1}). And we could find it showed better performance in the field of biosensing than the existing graphene-family composite including H-RGO-Au NRs. Compared with the previously reported methods, this strategy presents following advantages: First, the strategy did not need extra signal tag for sensing, and the carriers itself acted as signal which could provide large surface area for Con A as well as catalytic signal as artificial enzyme. Second, the newly-presented peroxidase mimetics H-RGO-Au NFs displays excellent catalytic ability which is expected to have bright prospects in clinic application.

Selectivity of the aptamer biosensing for K562 cells

Benefited by the specificity of the aptamer for cells, the biosensor is expected to hold good selectivity. Therefore the following experiments were carried out to find the selectivity of this system for K562 cells employing four kinds of cells including Hela cells (a line of human cells derived from cervical cancer), Romas cells (human lymphoma cell line), K562 cells and lung

cancer cells in human serum sample. The presented sensor was treated with above four kinds of cancer cells with concentrations of 10^4 cells mL^{-1}, and the CV response in H_2O_2 solution was measured respectively. At the same time, TMB-H_2O_2 system was used to intuitively show the color changes when employing different kind of cells. From the data displayed in Figure 6, we could find that the sensing electrode treated with K562 cells showed obvious catalysis signal during CV measurement. While, electrodes treated by three control groups (Hela cells, Romas cells and human lung cancer cells) did not show apparent signal change compared with blank control group (no cells were introduced into the electrode). This is attributed to the specific identification between the K562 cells and its aptamer. Meanwhile, the color changes due to the change of absorbance were captured by smartphone and showed as the insert of Figure 6. From the picture, we could also find that only K562-captured system showed obvious blue color, indicating the successful modification of H-RGO-Au NFs as catalyzer for the redox reaction of TMB-H_2O_2 system. This is in accord with the CV response and further confirmed the good selectivity of this aptamer biosensor.

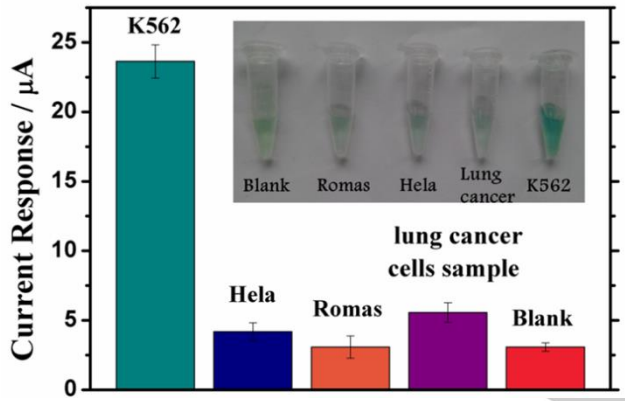

Figure 6. Selectivity analysis for K562 cells detection by monitoring CV signal of different kind of cancer cells. The concentration of cancer cells is 10^4 cells mL^{-1}. The error bars represent the standard deviation of three measurements. Insert is the representative photograph of four kinds of cancer cells modified electrodes in the peroxidase mimetic -mediated TMB-H_2O_2 system. The photos were taken after 5 min oxidation of TMB catalyzed by peroxidase mimetic H-RGO-Au NFs modified electrodes.

Conclusions

The presented biosensing platform employed newly-designed ternary composite H-RGO-Au NFs with enhanced catalytic ability for the detection of K562 cancer cells. This graphene-family ternary composite was first reported with prickly nanoflower morphology on its surface which greatly improved the performance as a peroxidase mimetics. Attributed to the large surface area of substrate graphene, unique morphology of Au NFs, as well as the synergistic interaction from hemin and gold nanomaterial, the presented composite showed better performance than that of previously-presented materials. This biosensor realized sensitive detection of K562 cells and it could be widely applied in sensitive and selective clinic detection for nucleic acid, protein, or cells in a convenient way.

Experimental Section

Materials.

Graphene Oxide dispersion (Nanjing XFNANO Materials Tech Co., Ltd.), Tris (2-carboxyethyethyl) phosphine hydrochloride, EDTA disodium salt dehydrate, 6-Mercapto-1-hexaol and 3,3′ ,5,5′ -Tetramethylbenzidine dihydrochloride hydrate (TMB) (Aladdin, China), Hydroxylamine hydrochloride (Sigma-Aldrich), Bovine serum albumin (BSA, Sigma-Aldrich), poly(diallyldimethylammonium chloride) (PDDA, Mw400 000500 000, 20 wt % in H_2O, Sigma), Hematin chloride (Shanghai Generay Biotech Co., Ltd), Concanavalin A (Solarbio) Chloroauric acid ($HAuCl_4{\cdot}4H_2O$) and ascorbic acid (Shanghai Chemical Reagent Co., China).
Aptamer:5'-SH– TTTTTTTTTTACAGCAGATCAGTCTATCTTCT CCTGATGGGTTCCTATTTATAGGTGAAGCTGT-3' (SBS Genetech Co.,Ltd).

Synthesis of H-RGO-Au nanoflowers (H-RGO-Au NFs)

Very simple steps were needed in the synthesis of H-RGO-Au NFs. And the route for syntheses partly referred to the literature with necessary modification.[35] First, 25 nm spherical gold seeds were synthesized as follows. 50 mL 0.25 mM aqueous $HAuCl_4$ in a 100 mL flask was brought to a boil under stirring, then 0.75 mL 1% sodium citrate solution was added for reaction until the solution became wine red in color.

50 mL 0.25 mM $HAuCl_4$ aqueous solutions (pH was adjusted to 11.0 by 1 mol L^{-1} NaOH solution) was mixed with 2 mL 0.0017 g mL^{-1} H-RGO solution, 0.7 mL 40 mM $NH_2OH{\cdot}$ HCl solution and 3.3 mL 3.75 mM gold seeds at 25 °C. After mild shaking, the color of the solution turned from pale pink to blue green

Synthesis of H-RGO-Au nanoparticles (H-RGO-Au NPs)

H-RGO-Au NPs was prepared using our previously reported method.[36] H-RGO-Au NPs was obtained by in situ reduction of $HAuCl_4$ with $NaBH_4$ and ascorbic acid (AA) with the presence of H-RGO. Spherical Au NPs were in situ grown on the surface of H-RGO to form H-RGO-Au NPs.

Synthesis of H-RGO-Au nanorods (H-RGO-Au NRs)

H-RGO-Au NRs were synthesized according to our previous method.[31] The seed solution was first prepared by mixing 1 mL 0.12 mM $HAuCl_4$ and 1 mL 0.048M CTAB solution. Another fresh prepared 0.12 mL 2.4 mM $NaBH_4$ was further added into Au (III)-CTAB solution with 2 min vigorous stirring. The solution color changed from yellow to brownish-yellow and aged at 27℃. Then the growth solution was prepared using 50 mL 0.2 mM $HAuCl_4$ gently mixed with 50 mL 0.048M CTAB, 2.5 mL 0.96 mM $AgNO_3$, 3.4 mg H-RGO product and 0.7 mL 0.01M AA. As the solution became colorless, 0.12 mL above prepared seed solution was gently added at 27℃ for 20 min and was kept for 12 h at 30℃ for nanorods' growth. The final product was re-dispersed in water after isolation by centrifugation at 8500 rpm for 25 min.

Preparation of Au/DNA biosensing surface

Gold disk electrode was polished by Al_2O_3 powder and electrochemically cleaned by numerous oxidation and reduction cycles in 0.5 M H_2SO_4. The cleaned gold electrode was dropped with 5 μL 10 mM Tris-HCl solution (pH 8.0) containing 1 μM aptamer DNA, 1.0 mM EDTA, 1.0 M NaCl and 1.0 mM TCEP for reaction 16 h at 4℃. The modified electrode was then treated with 1.0 mM MCH aqueous solution, and then was rinsed and dried with nitrogen for future use.

Cell culture and treatment

K562 cells (a human leukemic cell line), Hela cells (a line of human cells derived from cervical cancer), and Romas cells (human lymphoma cell line) purchased from Silver Amethyst Biotech. Co. Ltd. (Beijing, China) were cultured in a RPMI 1640 medium (GIBCO) in addition of fetal calf serum (10%, Sigma), penicillin (100 mg mL^{-1}), and streptomycin (100 mg mL^{-1}) at 37℃ in a humidied atmosphere of 5% CO_2. Cells in the exponential growth phase were collected after 5 min centrifugation at 1000 rpm followed by washing with sterile phosphate buffer saline (PBS, pH 7.4) twice. A Petroff-Hausser cell counter (U.S.A.) was used to obtain the cell concentration. Lung cancer cells in human serum sample were kindly given by Linyi cancer hospital.

Cell capture on biosensing surface

The modified electrode was immersed in 200 μL various concentrations of target K562 cells for 30 min at 37 °C under 5% CO_2. Then after removing the reaction solution, the electrode was rinsed and dried for further use.

Preparation of ConA/ H-RGO-Au NFs Conjugates

5 mL H-RGO-Au NFs was dispersed into a 1 mL 0.2% PDDA aqueous solution for sonication 30 min to obtain a homogeneous solution. Then after centrifugation and carefully washed with water, 100 μL the obtained PDDA-functionalized H-RGO-Au NFs was mixted with 100 μL 2.0 mg mL^{-1} Con A solution dissolved in PBS in advance for 25 min. Then, the mixture was stirring at room temperature for 1.5 h followed by 20 min centrifugation at 10000 rpm. The sediment was washed and re-suspended in 200 μL PBS containing 1 mM Ca^{2+} and 1 mM Mn^{2+} and stored at 4℃ for use.

Electrochemical and Colorimetric Measurement

Standard three electrode system with gold electrode as the working was employed refering to our previous work.[32] The electrochemical measurement was conducted on CHI660B workstation (CHI Instruments Co. Ltd., Shanghai, China) in a glass cell containing 2 mM H_2O_2 solution. The reaction solution was bubbled for 15 min with nitrogen in advance and cyclic voltammograms (CVs) were recorded ranging the potential from -0.6 V to 0 V with 10 mV s^{-1}scan rate.

For the colorimetric measurement, the electrodes were immersed in 200 μL TMB/H_2O_2 substrate. The reaction solution was characterized by UV−vis absorption spectra on a Cary 60 UV-vis spectrometer. Kinetic data were studied by measuring the the absorbance change at 652 nm with the change of TMB or H_2O_2 concentration in TMB/H_2O_2 reaction solution in the corresponding composite (H-RGO-Au NFs, H-RGO-Au NRs and H-RGO-Au NPs).

Acknowledgements

Financial support was provided by the National Natural Science Foundation of China (Grant Nos.: 21505065, 21535002, 21675074), the Shandong Provincial Natural Science Foundation (ZR2014BL023 and ZR2014BL026), State Key Laboratory of Analytical Chemistry for Life Science (SKLACLS1407) , and the “Innovation Team Development Plan” of the Ministry of Education Rolling Support(IRT_15R31).

Keywords: gold nanoflower • peroxidase mimetics • graphene• aptamer biosening • cancer cells

[1] W. Tan, M. J. Donovan, J. Jiang, *Chem. Rev.* **2013**, *113*, 2842-2862.
[2] D. Li, S. Song, C. Fan, *Acc. Chem. Res*. **2010**, *43*, 631-641.
[3] X. J. Chen, Y. Z. Wang, Y. Zhang, Z. H. Chen, Y. Liu, Z. L. Li, J. H. Li, *Anal Chem.* **2014**, *86*, 4278-4286.
[4] L. Tang, Y. Liu, M. M. Ali, D. K. Kang, W. Zhao, J. Li, *Anal. Chem*. **2012**, *84* 4711-4717.
[5] R. Freeman, X. Q. Liu, I. Willner, *J. Am. Chem. Soc*. **2011**, *133*, 11597–11604.
[6] Y. Qi, B. X. Li, *Chem. Eur. J.* **2011,** *17*, 1642-1648.
[7] J. A. Hansen, J. Wang, A. N. Kawde, Y. Xiang, K. V. Gothelf, G. Collins, *J. Am. Chem. Soc*. **2006**, *128,* 2228-2229.
[8] X. L. Zuo,; S. P. Song, J. Zhang, D. Pan, L. H. Wang, C. H. Fan, *J. Am. Chem. Soc.* **2007**, *129*, 1042-1043.
[9] J. Wang, Y. Shan, W. Zhao, J. J. Xu, H. Y. Chen, *Anal. Chem.* **2011**, *83*, 4004-4011.
[10] M. N. Stojanovic, P. D. Prada, D. W. Landry, *J. Am. Chem. Soc.* **2001**, *123*, 4928-4931.
[11] S. D. Jhaveri, R. K. Rick Conrad, E. J. Maglott, M. Bowser, R. T. Kennedy G. Glick,; A. D. Ellington, *J. Am. Chem. Soc.* **2000**, *122*, 2469-2473.
[12] X. H. Fang, A. Sen, M. Vicens, W. H. Tan, *Sensors and Actuators B: Chemical* **2003**, *4*, 829-834.
[13] H. Zhou, T. Q. Han, Q. Wei, S. S. Zhang, *Anal. Chem*. **2016**, *88,* 2976-2983.
[14] Q. Wang, L. Zhang, C. S. Shang, Z. Q. Zhang, S. J. Dong, *Chem. Commun*. **2016**, *52*, 5410-5413.
[15] Y. J. Jua, J. H. Kim, *Chem. Commun.* **2015**, *51,* 13752-13755.
[16] J. P. Wei, X. L. Chen, S. Shi, S. G. Mo, N. F. Zheng, *Nanoscale* **2015**, *7,* 19018-19026.
[17] Y. Q. Chang, Z. Zhang, J. H. Hao, W. S. Yang, J. L. Tang, *Sensors and Actuators B: Chemical* **2016**, *232*, 692-697.
[18] S. J. Liu, J. W. Fu, M. H. Wang, Y. Yan, Q. Xin, L. Cai, Q. Xu, *Journal of Colloid and Interface Science* **2016**, *469*, 69-77.
[19] C. Hou, Y. Wang, Q. H. Ding, L. Jiang, M. Li, W. Zhu, D. Pan, H. Zhu, M. Z. Liu, *Nanoscale* **2015**, *7*, 18770-18779.
[20] F. Yuan, H. M. Zhao, H. M. Zang, F. Ye, X. Quan, *ACS Appl. Mater. Interfaces* **2016**, *8*, 9855-9864.
[21] Y. J. Song, K. G. Qu C. Zhao, J. S. Ren, X. G. Qu, *Adv. Mater*. **2010**, *22*, 2206-2210.
[22] N. R. Nirala, S. Abraham, V. Kumar, A. Bansal, A. Srivastava, P. S. Saxena, *Sensors and Actuators B: Chemica.* **2015**, *218*, 42-50.
[23] N. Xu, J. P. Lei, Q. B. Wang, Q. H. Yang, H. L. Ju, *Talanta* **2016**, *150*, 661-665.
[24] Y. Tao, Y. Lin, Z. Huang, J. Ren, X. Qu, *Adv. Mater*. **2013**, *25*, 2594-2599.
[25] Y. Liang, Y. Li, H. Wang, J. Zhou, J. Wang, T. Regier, H. Dai, *Nat. Mater*. **2011**, *10*, 780-786.
[26] M. D. Stoller, S. Park, Y. W. Zhu, J. H. An, R. S. Ruoff, *Nano Lett.* **2008**, *8,* 3498-3502.
[27] Y. Jv, B. X. Li, R. Cao, *Chem.Commun*. **2010**, *46,* 8017-8019.

[28] L. N. Zhang, H. H. Deng, F. L. Lin, X. W. Xu, S. H. Weng, A. L. Liu, X. H. Lin, X. H. Xia, W. Chen, *Anal. Chem.* **2014**, *86*, 2711-2718.
[29] H. Wang, S. Li, Y. M. Si, N. Zhang, Z. Z. Sun, H. Wu, Y.H. Lin, *Nanoscale* **2014**, *6*, 8107-8116.
[30] X. C. Lv, J. Weng, *Sci. Rep*. **2013**, *3*, 3285-3294.
[31] J. Liu, X. Y. Xin, H. Zhou, S. S. Zhang, *Chem. Eur. J.* **2015**, *21*, 1908-1914.
[32] J. Liu, M. R. Cui, H. Zhou, S. S. Zhang, *Sci. Rep.* **2016**, *6*, 30577-30585.
[33] D. Feng, Z. Y. Gu, J. R. Li, H. L. Jiang, Z. Wei, H. C. Zhou, *Angew. Chem.* **2012**, *124*, 10453-10456.
[34] Y. J. Guo, L. Deng, J. Li, S. J. Guo, E. K. Wang, S. J. Dong, *ACS Nano.* **2011**, *5*, 1282-1290.
[35] L. Zhao, X. H. Ji, X. J. Sun, J. Li, W. S. Yang, X. G. Peng, *J. Phys. Chem. C.* **2009**, *113,* 16645-16651.
[36] X. Y. Xin, Y. Y. Yang, J. Liu, X. M. Wang, H. Zhou, B. Yu, *RSC Adv.* **2016**, *6,* 26203-26209.
[37] L. Gao, J. Zhuang, L. Nie, J. Zhang, Y. Zhang, N. Gu, T. Wang, J. Feng, D. Yang, S. Perrett, X. Yan, *Nat. Nanotechnol* **2007**, *2*, 577-583.
[38] Y. J. Song, K. G. Qu, C. Xu, J. S. Ren, . G. Qu, *Chem. Commun.* **2010**, *46*, 6572-6574.
[39] Y. Tao, Y. H. Lin, Z. Z. Huang, J. S. Ren, X. G. Qu, *Adv. Mater*. **2013**, *25,* 2594-2599.
[40] Z. H. Chen, Y. Liu, Y. Z. Wang, X. Zhao, J. H. Li, *Anal. Chem*. **2013**, *85*, 4431-4438.
[41] W. Cheng, L. Ding, S. J. Ding, Y. B. Yin, H. X. Ju, *Angew. Chem., Int. Ed.* **2009**, *48*, 6465-6468.
[42] J. J. Zhang, F. F. Cheng, T. T. Zheng, J. J. Zhu, *Anal. Chem.* **2010**, *82*, 3547-3555.
[43] E. Han, L. Ding, R. Qian, L. Bao, H. Ju, *Anal. Chem.* **2012**, *84*, 1452-1458.
[44] V. Mani, B. V. Chikkaveeraiah, V. Patel, J. F. Rusling, *ACS Nano*. **2009**, *3*, 585-594.
[45] H. Zhou, Y. Y. Yang, C. X. Li, B. Yu, S. S. Zhang, *Chem.-Euro. J.* **2014**, *20,* 14736-14743.

10.1002/chem.201604354

WILEY-VCH

Entry for the Table of Contents (Please choose one layout)

Layout 1:

FULL PAPER

Text for Table of Contents

a smart electrochemical aptamer biosensor for K562 cells was presented with good performance in selectivity and sensitivity employing a new graphene-family ternary composite with prickly Au nanoflower on its surface.

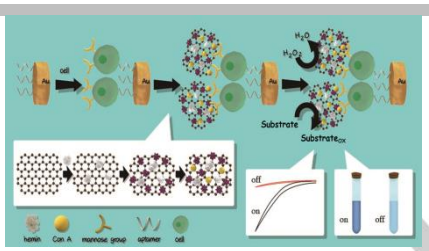

Jing Liu, Meirong Cui, Li Niu, Hong Zhou, Shusheng Zhang**

Page No. – Page No.

Title

Enhanced Peroxidase-like Properties of Graphene-hemin Composite Decorated Au Nanoflower and Application of Electrochemical Aptamer Biosensor for Detection of K562 Cells

Layout 2:

FULL PAPER

((Insert TOC Graphic here; max. width: 11.5 cm; max. height: 2.5 cm))

*Author(s), Corresponding Author(s)**

Page No. – Page No.

Title

Text for Table of Contents